

OPEN ACCESS

EDITED BY

Luisa M. P. Valente,
Universidade do Porto, Portugal

REVIEWED BY

Nor Azman Kasan,
University of Malaysia Terengganu,
Malaysia
Niels Bols,
University of Waterloo, Canada
Patricia Diaz-Rosales,
Centro de Investigación en Sanidad
Animal (CISA) (CSIC), Spain

*CORRESPONDENCE

Øystein Sæle
oystein.saele@hi.no
Chandrasekar Selvam
fishochand@gmail.com

SPECIALTY SECTION

This article was submitted to
Aquatic Physiology,
a section of the journal
Frontiers in Marine Science

RECEIVED 27 May 2022

ACCEPTED 12 September 2022

PUBLISHED 29 September 2022

CITATION

Selvam C, Saito T, Sissener NH,
Philip AJP and Sæle Ø (2022)
Intracellular trafficking of fatty acids in
the fish intestinal epithelial cell
line RTgutGC.
Front. Mar. Sci. 9:954773.
doi: 10.3389/fmars.2022.954773

COPYRIGHT

© 2022 Selvam, Saito, Sissener, Philip
and Sæle. This is an open-access article
distributed under the terms of the
[Creative Commons Attribution License
\(CC BY\)](https://creativecommons.org/licenses/by/4.0/). The use, distribution or
reproduction in other forums is
permitted, provided the original
author(s) and the copyright owner(s)
are credited and that the original
publication in this journal is cited, in
accordance with accepted academic
practice. No use, distribution or
reproduction is permitted which does
not comply with these terms.

Intracellular trafficking of fatty acids in the fish intestinal epithelial cell line RTgutGC

Chandrasekar Selvam^{1,2,3*}, Takaya Saito¹, Nini H. Sissener¹,
Antony J. Prabhu Philip¹ and Øystein Sæle^{1*}

¹Feed and nutrition, Institute of Marine Research, Bergen, Norway, ²Department of Biological Sciences (BIO), University of Bergen, Bergen, Norway, ³Marine Biotechnology, Fish Nutrition and Health Division, Central Marine Fisheries Research Institute, Kochi, India

The shift towards higher inclusion of vegetable oils (VOs) in aquafeeds has resulted in major changes in dietary fatty acid composition, especially increased amounts of monounsaturated fatty acids (MUFAs) and decreased polyunsaturated fatty acids (PUFAs) and saturated fatty acids (SFAs). However, little is known about how this change in fatty acid (FA) profile affects the intracellular fate of these fatty acids in the intestinal cells. To investigate this topic, we used the rainbow trout intestinal epithelial cell line (RTgutGC) as an *in vitro* model. The cells were incubated with either palmitic acid (16:0, PA), oleic acid (18:1n-9, OA), or arachidonic acid (20:4n-6, ARA), to represent the SFA, MUFA, and PUFA, respectively. In all experiments, the RTgutGC were incubated with either non-labeled or radiolabeled FA (PA, OA, or ARA) for 16 h at 19°C. The cells were then analyzed for the occurrence of cytosolic lipid droplets (CLD) with confocal microscopy, transcriptomic analysis (non-labeled FA experiments) and lipid class composition in the cells and serosal media from the basolateral side of the cells (radiolabeled FA experiments). CLD accumulation was higher in RTgutGC exposed to OA compared to cells given PA or ARA. This was coupled with increased volume, diameter, and surface area of CLDs in OA treated cells than with other FAs (PA, ARA). The results from radiolabeled FAs performed on permeable transwell inserts showed that OA increased the triacylglycerides (TAG) synthesis and was primarily stored in the cells in CLDs; whereas a significant amount of ARA was transported as TAG to the basolateral compartment. A significant proportion of free FAs was found to be excreted to the serosal basolateral side by the cells, which was significantly higher for PA and OA than ARA. Although there were clear clusters in differentially expressed genes (DEGs) for each treatment group, results from transcriptomics did not correlate to lipid transport and CLD analysis. Overall, the accumulation of TAG in CLDs was higher for oleic acid (OA) compared to arachidonic acid (ARA) and palmitic acid (PA). To conclude, carbon chain length and saturation level of FA differently regulate their intracellular fate during fatty acid absorption.

KEYWORDS

RTgutGC, fatty acids transport, lipid accumulation, cytosolic lipid droplets, triacylglycerides

Introduction

As opposed to most vertebrates, dietary triacylglycerides (TAG) are completely hydrolyzed in most teleost fish (Bogevik et al., 2008). The absence of monoacylglycerol as a digestive product in these fish is a consequence of the evolutionary loss of colipase (Sæle et al., 2018). Digested dietary fat is taken up by enterocytes, re-esterified into complex lipids in the endoplasmic reticulum and subsequently directed to synthesis of lipoproteins for transport or stored in cytosolic lipid droplets (CLDs) (Sire et al., 1981; Sheridan, 1988; Sigurgisladdottir et al., 1992; Bogevik et al., 2008). CLDs are temporary lipid storage molecules, consisting of a core of neutral lipids, mostly TAG and esters, surrounded by monolayer phospholipids. It has been shown that high lipid diets increase the number and size of CLDs. Moreover, replacing fish oil with vegetable oils (VOs) could also influence the CLD accumulation (Deplano et al., 1989; Olsen et al., 1999; Olsen et al., 2000; Caballero et al., 2002; Caballero et al., 2003). Although CLDs are considered as temporary lipid storage organelles, they serve several crucial physiological functions, including sequestering toxic lipid molecules and preventing lipotoxicity, maintenance of endoplasmic reticulum membrane homeostasis, regulation of fatty acid (FA) storage, and transport (Walther and Farese, 2012; Olzmann and Carvalho, 2019). However, excessive accumulation of CLDs may also cause damage to the cells and create pathogenicity (Schaffer, 2003). For instance, studies in Arctic char (*Salvelinus alpinus*) and rainbow trout (*Oncorhynchus mykiss*) have demonstrated extensive damage to enterocytes due to excessive accumulation of CLDs caused by VO diets high in monounsaturated fatty acids (MUFA) (Olsen et al., 1999; Olsen et al., 2000; Olsen et al., 2003).

Due to the loss of colipase in fish, dietary TAG is completely hydrolyzed to single fatty acids (FAs). This leaves the monoacylglycerol pathway without substrate and all absorbed FAs are resynthesized into TAG *via de novo* synthesis and ultimately transported into CLDs within the enterocytes. We hypothesize that chylomicrons/VLDL (very low-density lipoprotein) can be generated for export only after the synthesis and storage of TAG within lipid droplets. Further, we hypothesize that the intracellular trafficking of FAs in the enterocytes is affected by carbon chain length and saturation, hence there will be consequences of changing the dietary FA composition. Therefore, the present work is aimed to study the effects of carbon length and unsaturation levels on intracellular lipid trafficking and CLDs formation *in vitro* using RTgutGC (Rainbow trout gut cell). The current study used three different approaches: (i) live-cell imaging for lipid droplets formation, (ii) radiolabeled FAs for lipid class analysis, and (iii) whole cell transcriptomic analysis. The FAs chosen for the current study were palmitic acid (PA), oleic acid (OA), and arachidonic acid (ARA), to represent the saturated fatty acid (SFA), MUFA, and polyunsaturated fatty acid (PUFA), respectively. These FAs were selected based on their relevance to current feeding practices in

salmonids aquaculture. In particular, increased use of vegetable oils in fish feed has resulted in decreased dietary n-3 PUFA and SFA (PA); and increased n-9 (MUFA) and n-6 PUFA.

The RTgutGC cell derived from rainbow trout intestine exhibits apical and basolateral characteristics of intestinal epithelial cells (Kawano et al., 2011). It has been proposed as a physiologically adequate fish intestinal epithelial model, which is equivalent to human intestinal epithelial cells (Caco2 cells) (Kawano et al., 2011; Minghetti et al., 2017). In addition, RTgutGC contains functionally active polarized absorptive cells (enterocytes) that play a central role in lipid metabolism. In general, enterocytes are responsible for assimilation of luminal FAs and also support the *de novo* synthesis of FAs and cholesterol and serve as a site for production of major lipid transport proteins such as apolipoproteins. Recently, the RTgutGC cell line has been used as a model to study nutrient uptake (Antony Jesu Prabhu et al., 2018; Kim et al., 2018; Pumptis et al., 2018), test functional ingredients and gut immune function (Wang et al., 2019; Holen et al., 2021) and toxicity (Langan et al., 2017; Schug et al., 2020). To our best knowledge, most studies of FA uptake and trafficking by intestinal epithelial cells were conducted in immortalized cell lines such as Caco2 and IEC-6 as enterocyte models. Furthermore, FA uptake and transport system in fish were largely studied *in vivo*, where dietary lipids are more complex, and finding the fate of individual FA is more onerous. Thus, the current study would be the first trial using fish enterocyte cell model (RTgutGC) to study the intracellular lipid trafficking and CLDs formation in fish intestinal epithelial cells.

Materials and methods

Routine RTgutGC cell culture

The intestinal epithelial cell line from rainbow trout (RTgutGC) was obtained from the Swiss Federal Institute of Aquatic Science and Technology (Eawag), Switzerland, through a material transfer agreement. RTgutGC cells were routinely cultured as per the methods described by Kawano et al. (2011). In brief, cells were grown in a 75 cm² culture flask with Leibovitz' L-15 complete medium (21083027, Gibco Thermofisher), supplemented with 10% fetal bovine serum (F7524, Sigma Aldrich) and 1% Antibiotic Antimycotic Solution (A5955, Sigma Aldrich) maintained at 19°C under normal atmosphere. After reaching confluency in 7-10 days, cells were sub-cultured for routine maintenance as per the method described by Kawano et al. (2011), or harvested to be used in experiments.

Preparation of FA - BSA complexes

The non-radio labeled palmitic acid (PA, P0500, Merk), oleic acid (OA, O1008, Merk), or arachidonic acid (ARA, 10931,

Merk) were conjugated to FA-free bovine serum albumin (BSA, A6003, Sigma Aldrich), as per the method previously described by Nøstbakken et al. (2012). In brief, an appropriate amount of FA was weighed in a dark glass container to yield 3.46 mM concentration, and 0.04 ml chloroform per mg FA was added to completely dissolve the FA. After evaporating chloroform under the N₂ stream, the residue was dissolved in 0.124 M KOH at the ratio of 1:3 and vortexed continuously for 10 min. FA free-BSA (1.5 mM) dissolved in serum-free culture media (Leibovitz' L-15) was added in a 2.5:1 molar ratio to the FA and stirred continuously in water bath for 45 min at 37°C. The final concentration of FA was 3.46 mM, filter sterilized and stored in -20°C until use.

Lipotoxicity test using xCELLigence system

The lipotoxicity effects of FA in RTgutGC were carried out according to the methods described by (Berger et al., 2017). In brief, the E96 xCELLigence plate was prepared by adding 50 µl of culture media to each well and incubating in xCELLigence for 30 minutes with background corrections. The cells were seeded at a density of 20,000 cells/well in 100 µl culture media. The cell adhesion and proliferation were monitored every 15 min by the xCELLigence system. Approximately 24 h after seeding, when the cells were in the log growth phase, the cells were exposed to 50 µL of medium containing the BSA conjugated FA (PA, OA, or ARA) at concentrations 50-1000 µM in triplicate, and the experiments were continued for another 24 h. Controls received either medium only or medium + BSA.

Visualization of intracellular lipid droplets and image analysis

RTgutGC cells were seeded on µ-slide 8 well plates with a chambered coverslip (Ibidi GmbH, 80826) at a density of 1.5 x 10⁵ cells/ml and incubated at 19°C for 48 h prior to FAs treatment. Cells were then washed twice with PBS and incubated with 200 µMFAs (PA, OA, or ARA) conjugated with BSA for 16 h at 19°C. BSA in serum-free cell culture media but no FA was used as a control. After the incubation, cells were washed twice with PBS and incubated with LipidSpotTM 488 (green) lipid droplet stain (1:1000) (Biotium, 70065-T) in complete cell culture medium at 19°C for 30 min as per the manufacturer's instructions, protected from light prior to imaging. Visualization of lipid droplets was achieved by Ti-E inverted microscope (Nikon, Japan) with a CFI Super Plan Fluor ELWD ADM 20 X C PH-1 objective, numerical aperture 0.45 (Nikon, Japan), and a C2 + confocal scanner (Nikon, Japan). Images were acquired using an oil immersion 60× objective, and Z-stacks were taken with a defined Z-step size of 0.93µm and

1024 x 1027 pixels. All the acquired 3D constructions were background-subtracted and analyzed using NIS Elements AR v.4.51 (Nikon, Tokyo, Japan) software to obtain data on CLDs. The total number of CLDs per cell, and the volume, diameter, surface area, and sphericity of individual CLDs were obtained. In addition, the percentage of cells that accumulated CLDs was also analyzed manually, using a minimum threshold of 5 CLDs per cell. Three independent experiments were conducted, representing 3 replicates (n=3). Each experiment consisted of three wells for each FA (PA, OA, or ARA) and the control group.

Lipid class analysis in RTgutGC exposed to radiolabeled FAs

Preparation of uptake medium

The radiolabeled ³H-Palmitic acid (9,10-³H(N), NET043001MC, 1mCi, PerkinElmer), ³H-Oleic acid (9,10-³H(N), NET289001MC, 1mCi, PerkinElmer) and ³H-Arachidonic acid (5,6,8,9,11,12,14,15-³H(N), NET298Z050UC, 50µCi, PerkinElmer) were conjugated to non-radiolabeled FA-BSA stock solution as described earlier. An appropriate amount of radiolabeled FAs [³H] was taken in a dark glass tube and dried under N₂ gas, and BSA conjugated FA (3.46 mM) was added, followed by sonication in a water bath sonicator for 1 hr. In all the cases, the final working media contained ~200 µM FAs with radioactive concentration 1µCi/ml (~37 kBq/ml) and specific activities of 0.33 mCi/mmol for each FA.

Cell culture on permeable membranes

RTgutGC cells from routine culture flasks were trypsinized, counted and were seeded at a density of 75,000 cells/cm² onto apical compartment of 6 wells in commercially available permeable transwell-membrane inserts (ThinCert[®] cell culture inserts, pore size = 0.4 µm; polyethylene terephthalate [PET] from Greiner Bio-One, Germany) as described previously (Geppert et al., 2016; Minghetti et al., 2017). The apical and basolateral compartments were filled with 2 and 3 ml of complete L-15 culture media, respectively, and the culture media from both the apical and basolateral compartments were changed once every 3 days. The cells were grown for 18 days at 19°C before the experiments. The transepithelial electric resistance (TEER) was measured to assess the tightness of the cell monolayers by using the epithelial volt-ohm meter (EVOM) with dual "chopstick" electrodes (World Precision Instruments, New Haven, CT), and TEER values were calculated as per the method described by Geppert et al. (2016).

Incubation with radiolabeled FAs

RTgutGC cells grown on permeable transwell-membrane inserts were taken out of the incubator, and the medium from apical and basolateral sides was removed. The cells (apical side) were washed twice with PBS and then cells were incubated with FA

by replacing apical medium with 2 ml of medium containing FA conjugated with BSA with a final concentration of about 200 μM (PA, OA or ARA), containing 1 $\mu\text{Ci/ml}$ labeled FAs [^3H]; specific activities 0.33 mCi/mmol). The basolateral medium was replaced with serum-free medium containing only BSA. The cells were incubated for 16 h at 19°C. After the incubation period, samples (medium from the apical compartment, basolateral compartment, and the cells along with membrane) were collected in chloroform: methanol solution (1:1) for lipid extraction.

Lipid extraction and thin-layer chromatography

Thin-layer chromatography (TLC) was used to determine the type of lipids being secreted basolaterally from the cells following apical exposure to [^3H] FAs. Firstly, lipids from each sample were extracted by Folch's liquid-liquid extraction method using chloroform solvent. After phase separation, the aqueous phase was removed and discarded, and the remaining total organic extract was evaporated under a gentle stream of N_2 prior to TLC analysis. Extracted lipid was spotted on thin-layer chromatography plates (20 cm x 10 cm, Silica Gel) and developed in hexane-ethyl ether-acetic acid (80:20:1). Lipid standards consisting of triacylglycerides (TAG), free-fatty acids, and cholesterol were included in the analysis. The plates were developed with iodine vapor and the spots corresponding to TAG and FFA were scraped off into 20 ml scintillation vials and dissolved in 3 ml dichloromethane plus 15 ml ultima gold scintillation liquid. The amount of radioactivity [^3H] was measured in a scintillation counter (Packard Tri-Carb Liquid scintillation counter, Model 1900TR). The final concentration of each FA was calculated as follows,

$$\text{FA concentration (pmol)} = \frac{\left(\frac{\text{DPM}}{a} \times b \times 10^{12}\right)}{\text{SA}}$$

Where,

DPM, Disintegrations per minute

a= 60, conversion factor for DPM to becquerel (Bq)

b= 2.7×10^{-11} , conversion factor for becquerel to curie

SA, radioactive specificity of FA (mCi/mmol)

Transcriptomic analysis of RTgutGC cell exposed to different FAs

The RTgutGC cells were seeded in 6-well conventional culture plates at a density of 1.5×10^5 cells/ml in complete L15/FBS medium and incubated at 19°C for 3 days to reach the confluency (~80%). Subsequently, the medium was removed from the cells and then the cells were washed twice with PBS before treating with FAs. The FA (PA, OA, or ARA) conjugated with BSA (as described earlier) was added to the cells at a concentration of 200 μM and incubated at 19°C for 16 h. After exposure to the respective FAs, the medium was removed, and 0.4 mL of RTL lysis buffer (Qiagen, Germany) was added for 30s. The cell lysates were transferred to

2 ml tubes and stored in -80°C freezer until required for RNA isolation. Three independent parallel experiments were conducted, representing 3 replicates and n=9 for each FA (PA, OA, and ARA) and the control group.

RNA extraction

RNA isolation was performed with the RNeasy Plus Mini Kit including genomic DNA eliminator columns (Qiagen, Germany). Three independent parallel experiments were conducted, representing 3 replicates and n=9 for each FA (PA, OA, and ARA) and control group. RNA concentration and purity were measured using a Nanodrop Spectrophotometer (NanoDrop[®], ND-1000, Thermo Fischer, USA). Integrity of RNA was checked for all the samples using bioanalyzer as per the method provided by manufacturer (Agilent 2100 Bioanalyzer, Agilent Technologies, Palo Alto, CA, USA). All the samples except one sample from OA treatment group, had RIN values above 8.0 and were used for cDNA library preparation.

Library preparation and sequencing for RNA-seq

Library preparation and RNA-sequencing (RNA-seq) were performed by Novogene's UK Sequencing Centre, Cambridge, UK. The messenger RNA was purified from total RNA using poly-T oligo-attached magnetic beads. After purified RNA was fragmented, the first strand cDNA was synthesized using random hexamer primers followed by end repair, A-tailing, adapter ligation, size selection, amplification, and purification. The library was checked with Qubit and real-time PCR for quantification and bioanalyzer for size distribution detection. RNA-seq libraries were sequenced on Illumina Novaseq 6000 platform, where 150-bp paired-end reads were obtained. The raw RNA-Seq data were deposited and released in the sequence read archive database, with the BioProject accession number of PRJNA763330.

Rainbow trout genome and genomic annotation

The reference sequence data (Omyk_1.0) were downloaded from the NCBI assembly site (https://www.ncbi.nlm.nih.gov/assembly/GCF_002163495.1).

Quality trimming, alignment and quantification of RNA-seq reads

Adaptors, low-quality bases, low-quality reads (phred scores < Q30) and reads less than 20 bases in length were trimmed from

sequence reads using cutadapt (Martin, 2011). Quality trimmed reads were aligned to the Rainbow trout RefSeq reference genome (Omyk_1.0). STAR (Dobin et al., 2013) was used with the default parameters to index the reference genome and align reads to the indexed genome. The number of reads per gene was quantified using featureCounts (Liao et al., 2014), based on genomic coordinates provided by the general feature format (GFF) file from the Omyk_1.0 reference genome. The number of the reads that uniquely mapped on protein-coding genes was 68.7% in average (Table S1). The precomp function of R (<https://CRAN.R-project.org>) was used to perform principal component analysis (PCA) prior to differential expression analysis.

Differential gene expression analysis

Differential expression analysis was performed in a pair-wise manner by comparing three different FAs (PA, OA, or ARA) against the control group using the DESeq2 package (Love et al., 2014). The minimum log fold change (lfc) was set to $\log_2(1.5)$ using the lfcThreshold option in the results function to ensure that all DEGs were $>\log_2(1.5)$ and $<-\log_2(1.5)$. After p-values were adjusted by the Benjamini-Hochberg procedure, genes were identified as differentially expressed genes (DEGs) when adjusted p-values were less than 0.1. Heatmaps of overlapped DEGs were generated with the Complex Heatmap package (Gu et al., 2016). The in-house RNA-seq workflow was coordinated in a pipeline by Snakemake (Koster and Rahmann, 2012) with various R and Python scripts along with multiple bioinformatics tools.

Statistical analysis

Statistical analysis was performed using the software Statistica 13.4 (Statsoft Inc., Tulsa, OK, USA) and GraphPad Prism version 8.0 (Graphpad Software Inc., San Diego, CA, USA). Data were tested for normality and homogeneity of variance using the Kolmogorov-Smirnov test and Shapiro-Wilk test. Data were analyzed by one-way ANOVA, and comparisons between FAs were performed using Tukey's *post-hoc* analysis. Three independent experiments were conducted for CLDs analysis and transcriptomics studies, and two experiments were done for radiolabeled lipid class analysis. All experiments were performed in triplicate and values are expressed as mean \pm SEM.

Results

Lipotoxicity test

The lipotoxicity test was performed for the FAs (PA, OA, and ARA) conjugated with BSA in the range of 50-1000 μM (Figure 1). The strength of cell adhesion is represented as the

Cell Index (CI) which is a unit-less measurement. The cell index of cells beginning from 20,000 cells/well increased as the cell number increased. The CI was normalized at the time point before FA was added. The RTgutGC exposed to different concentration of FA (PA, OA, or ARA) grew continuously irrespective of FA concentration (50, 100, 200, 300, 400, 600, 800 and 1000 μM). However, there was significant reduction in cell index for cells exposed to higher concentration (800 and 1000 μM ; $P < 0.05$). Further, cell peak growth was observed between 200-300 μM and 200 μM was chosen for all the FA exposure experiments.

Intracellular cytosolic lipids droplets

The intracellular CLDs formation was significantly influenced by FAs supplementation in culture media (Figure 2A). The percentage of cells that accumulated CLDs was significantly different between treatments ($P < 0.0001$), and the highest percentage was found for OA ($97 \pm 0.9\%$) followed by ARA ($52 \pm 3.6\%$), PA ($34 \pm 3.6\%$), and then control ($13 \pm 3.0\%$) (Figure 3A). The number of CLDs accumulated per cell was significantly ($P < 0.0001$) higher for OA (117.8 ± 7.7) compared to PA (21.10 ± 1.3), ARA (26.6 ± 2), and control (11.6 ± 1.0) and no significant differences were found between PA vs ARA ($P = 0.77$) (Figure 3B). Subsequently, the mean volume of the CLDs was also significantly ($P < 0.0001$) higher for OA (2.8 ± 0.2) compared to PA (0.62 ± 0.03), ARA (0.76 ± 0.06), and the control (0.52 ± 0.02) (Figure 3C). The surface area of the CLDs (Figure 3D) was significantly ($P = 0.0001$) higher for cells supplemented with OA (12.8 ± 0.5) compared to PA (4.7 ± 0.2), ARA (4.7 ± 0.2) and the control (3.9 ± 0.14). Likewise, the diameter of the CLDs (Figure 3E) was also significantly ($P = 0.0001$) higher for cell treated with OA (1.2 ± 0.01) than compared to other treatment groups (PA, 0.86 ± 0.01 ; ARA, 0.80 ± 0.001 ; Control, 0.79 ± 0.0001). The sphericity of the CLDs (~ 0.7) was similar for all treatment groups (Figure 3F).

Lipid classes during FA transport

TEER levels increased and stabilized at an average of $33 \Omega \text{ cm}^{-2}$ after 18 days of culture with significant difference observed over time (Figure 4). TEER values reached a stable plateau at approximately 8-10 days. Cells seemed to stop proliferating but remained viable. The total amount of [^3H] FFA and [^3H] TAG was measured from the three fractions, i.e., apical, basolateral, and as well as cells on the permeable membrane (Figures 5, 6). The percentage of [^3H] labeled FAs recovered from FFA and TAG fractions were 91.3 ± 2.1 , 58.7 ± 7.0 , and $56 \pm 7.6\%$ for OA, PA, and ARA respectively (Figure 6). The saturation level of the added FA significantly influenced the uptake of FA from the apical medium by the cells. The amount of recovered [^3H] labelled FFA from the apical medium was similar for ARA

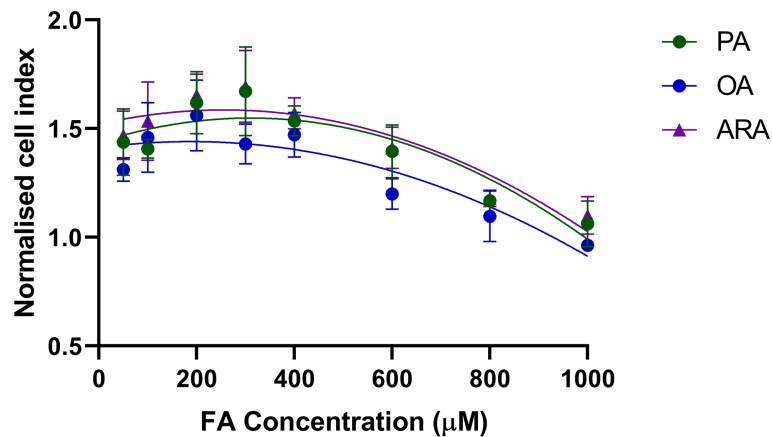


FIGURE 1

Normalized cell index of RTgutGC cells exposed to FA (PA, OA, or ARA). Cells were seeded at a density of 20,000 cells/well in a 96-well E-plate allowing the cells to adhere and proliferate for 24 h. Cells were then exposed to FA (PA, OA, or ARA) conjugated with BSA complex in the range of 50 – 1000 µM and monitored for 24 h using an xCELLigence system. Data shown here are cell adhesion as mean normalized cell index at 24 h exposure. PA, Palmitic acid; ARA, Arachidonic acid; OA, Oleic acid.

(347.9 ± 7.3 pmol; 50.4%) and PA (346.2 ± 4.7 pmol; 51.1%), while a numerically higher amount was observed for OA (512.4 ± 14.7 pmol; 73.5%); however, no significant difference was observed between them due to variation between the trials ($P=0.3$) (Figures 5A, 6). The amount of recovered [^3H] FFA from the basolateral medium was significantly higher for PA (19.3 ± 1.4 pmol, $P=0.02$; 3.5%) and OA (17.9 ± 1.0 pmol,

$P=0.03$; 3%) compared to ARA (5.3 ± 0.3 pmol; 1.1%), with no significant difference found between PA and OA ($P=0.8$) (Figures 5B, 6). Although similar trends were seen for the [^3H] FFA recovered from the cell fraction, no significant difference was observed among FAs treatments ($P=0.29$) (Figure 5C). Similarly, the amount of [^3H] recovered as TAG was measured for the medium from the apical and basolateral compartments,

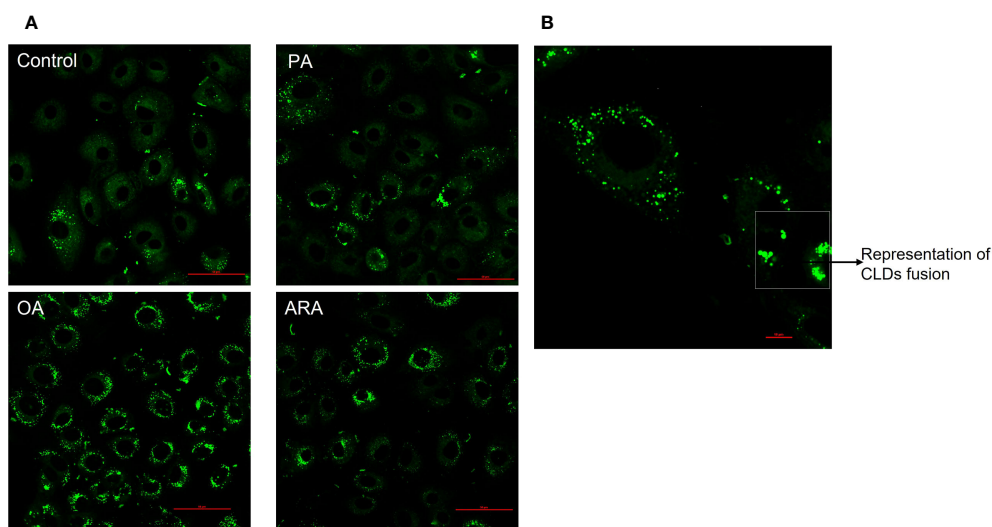


FIGURE 2

FAs differentially regulate lipid droplets accumulation in RTgutGC cells. (A) Representative confocal imaging of RTgutGC cells treated with 200 µM of FAs (PA, OA or ARA) control for 16 h at 19°C and stained with LipidSpotTM 488 (green); Scale bar: 50 µm. (B) Representative image of CLDs fusion in RTgutGC cells treated with 200 µM of oleic acid; scale bar: 10 µm. Scale bar: 10 µm. All images were acquired using an oil immersion 60× objective, and Z-stacks were taken with a defined Z-step size of 0.93 µm and 1024 X 1027 pixels. PA, Palmitic acid; ARA, Arachidonic acid; OA, Oleic acid.

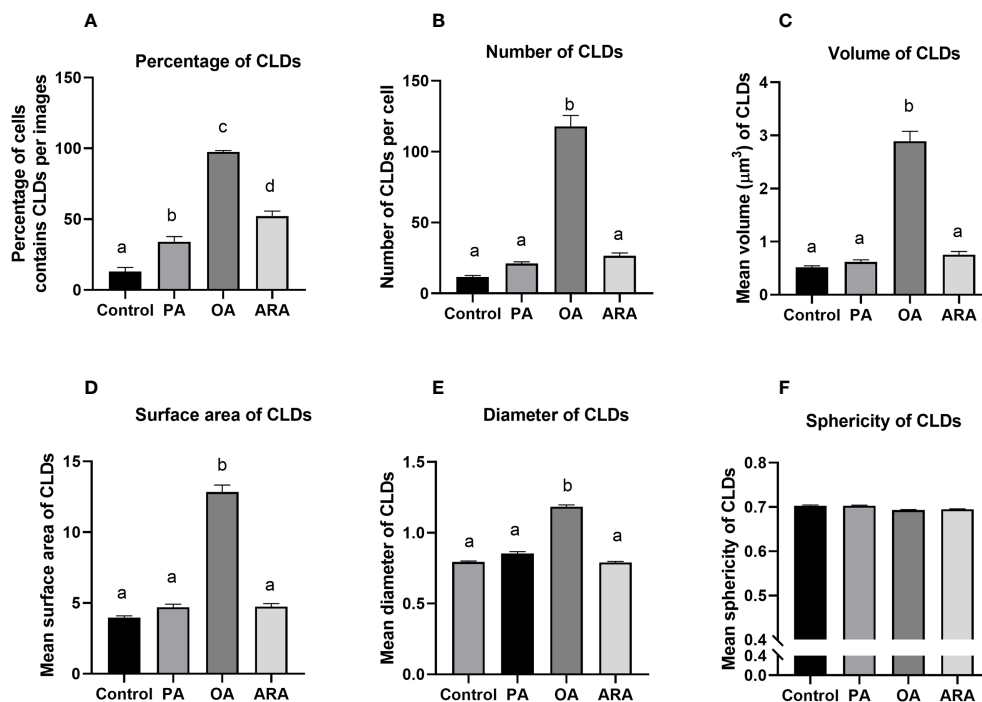


FIGURE 3

Quantification of CLDs accumulated in RTgutGC cells treated with 200 μM of FAs (PA, OA or ARA) and control for 16 h at 19°C and stained with LipidSpot™ 488 (green). The Percentage of cells contained CLDs per images (A), number of CLDs per cell (B), mean individual volume (C), surface area (D), diameter (E), and sphericity (F) of CLDs in RTgutGC cells. Different superscript (small letters) indicates statistical significance as obtained through one-way ANOVA followed by Tukey's multiple comparisons. Data are from $N = 18$ images analyzed from three independent experiments and are shown as mean \pm SEM. PA, Palmitic acid; ARA, Arachidonic acid; OA, Oleic acid.

and the cells. The cells supplemented with ARA had a significantly higher amount of [^3H] TAG in the basolateral compartment (4.1 ± 0.3 pmol, $P=0.006$; 1.1%) compared to PA (0.12 ± 0.03 ; 0.03%) and OA ($P=0.34 \pm 0.12$; 0.05%), with no differences between the latter two groups ($P=0.9$) (Figures 5E, 6). Conversely, the cell fraction had a significantly higher amount of [^3H] TAG for the group supplemented with OA (72.7 ± 10.3 pmol, $P=0.005$; 13.8%) compared to PA (20.6 ± 1.2 pmol; 3.3%) and ARA (13.1 ± 0.2 pmol; 2.8%), and no differences were found between the latter two groups ($P=0.56$) (Figures 5F, 6). There was no difference in [^3H] TAG content found in the apical fraction between the FAs ($P=0.57$; Figure 5D).

Transcriptomics

A summary of total RNA-seq reads generated for each sample, the corresponding STAR alignment results, and the alignment count data can be found in supplementary file 1. In general, transcriptomics analysis was performed on 35 samples of RTgutGC cells incubated for 16 h with their respective FAs conjugated with BSA (control, PA, OA, or ARA). Approximately,

21.2 to 30 million paired-end reads were obtained per sample. The results of the principal component analysis (PCA) with the normalized counts (Figure 7A) showed that PA group was distinctly separated to control group with OA and ARA being intermediary and overlapping with each other. Further, the differentially expressed genes (DEGs) were calculated as log fold changes [$\text{log}_2 \geq 2(1.5)$] along with the P-values (adjusted P-value of 0.1) by comparing FAs (PA, OA, or ARA) against control. The DEGs analysis revealed a total of 1294, 459, and 249 DEGs for PA, ARA, and OA, respectively. Out of that, 114, 26, and 55 DEGs were shared by every combination of two groups, namely PA and ARA, PA and OA, OA and ARA, respectively. Concurrently, 1003, 139, and 17 were explicitly expressed in PA, ARA, and OA, respectively (Figure 7B).

A total of 489 target genes involved in FAs absorption, transport, lipid droplet synthesis, FA synthesis and oxidation, TAG synthesis and hydrolysis, phospholipid synthesis, etc., were selected by using the rainbow trout gene database (NCBI, Ensemble) (See supplementary file 2 for a full list of genes analyzed). Out of 489 analyzed target genes, more DEGs were observed in the ARA treatment group (6.5%; 32 DEGs), followed by OA (4.1%; 20 DEGs) and PA (3.7%; 18 DEGs) (Figure 8),

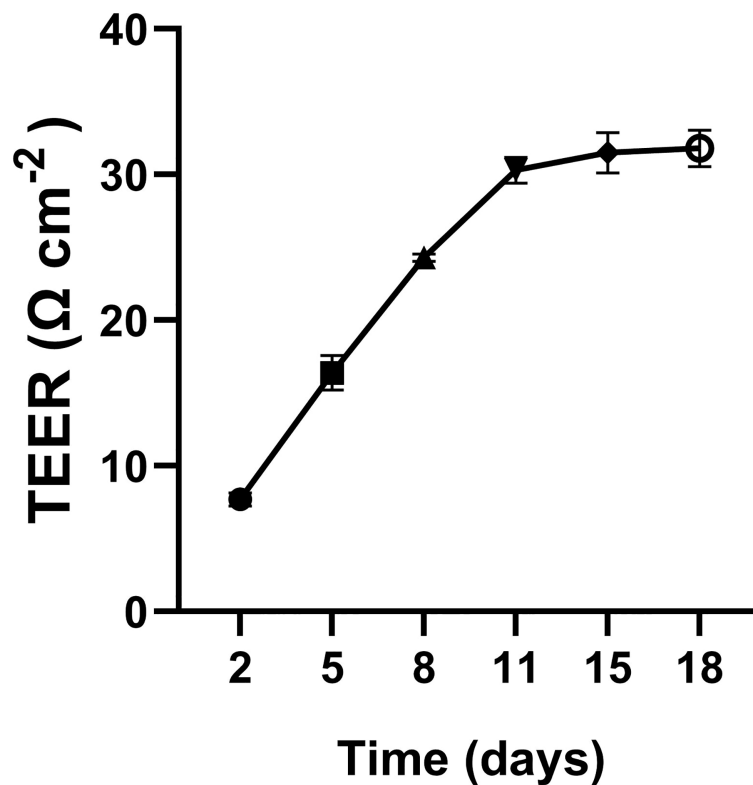


FIGURE 4

Trans epithelial electrical resistance (TEER) of RTgutGC cells. Cells were seeded at a density of 75,000 cells/cm² on transwell membrane inserts (0.4 μm pore size) and grown for up to 18 days.

when compared to control group. A heatmap was constructed for selected target genes that were identified as DEGs (Figure 8). Several transcripts involved in FA uptake and activation (lfc ≥ 1.5 , *fatp1-like-1*, *fatp1-like-2* and *abcf2a9*) were significantly upregulated in all FA supplement groups. Among the transcripts related to the TAG synthesis pathway that were analyzed, more DEGs (10) were identified in the PA group, and most of them were upregulated. On the other hand, the TAG synthesis pathway was downregulated (5 out of 6 DEGs) in OA and ARA. However, transcripts involved in TAG hydrolysis (*lpl-like-1*, *lpl-like-2*, and *pnpla2-like1*) were more downregulated in ARA followed by OA and PA. Further, the expression of *mttp*, a key protein involved in chylomicron assembly, was significantly upregulated in all FA groups compared to control group, however, this expression was significantly higher in PA (lfc, 1.49) than ARA (lfc, 1.12) and OA (lfc, 1.03). Surprisingly, no other transcripts involved in lipoprotein synthesis were differentially expressed except *sar1b* upregulation in ARA and OA. Associated with lipid droplet formation, out of 7 analyzed *plin* transcripts (*plin 1*, *plin 2*, *plin 3*, and *plin 6*), two transcripts from *plin 2* (*plin-2like1*; *plin-2 like2*) had differential expression

and were significantly upregulated in all groups. Furthermore, the upregulated *plin 2* was higher in PA (*plin-2like1*, lfc 6.1; *plin-2like1*, lfc 3.5) than in ARA (*plin-2like1*, lfc 5.1; *plin-2like1*, lfc 3.1) and OA (*plin-2like1*, lfc 4.2; *plin-2like1*, lfc 3.1) groups. However, none of the transcripts in apolipoprotein synthesis were differentially expressed. In particular, very low expression was observed for Apo B. On the other hand, expression of *apoa I-IV*, *apoc*, *apod* and *apoE* was prominent, but no DEGs. More downregulated transcripts involved in FA synthesis (*acsl4a*, *acsbg2*, *acs like-1*, *acs like-2*, *fasn-like-1*, *fasn-like-1*, *acac*) were observed in ARA and OA, and their downregulation was higher in ARA compared to OA. Whereas transcripts involved in FA synthesis (*acsl4a*, lfc 0.5; *acsbg2*, lfc 0.9; *scd*, lfc 0.6, *acot1-like*, lfc 2.1) were upregulated in PA. In respect to the β -oxidation pathway, more upregulated DEGs were identified in all FAs groups, and the upregulation was significantly higher in the ARA group than compared to OA and PA, and the lowest expression was observed in PA. Interestingly no analyzed transcripts involved in endoplasmic reticulum (ER) stress (*edem*, ER degradation enhancer, mannosidase; *hsp70*, Heat shock protein 70) were significantly affected by FAs supplements.

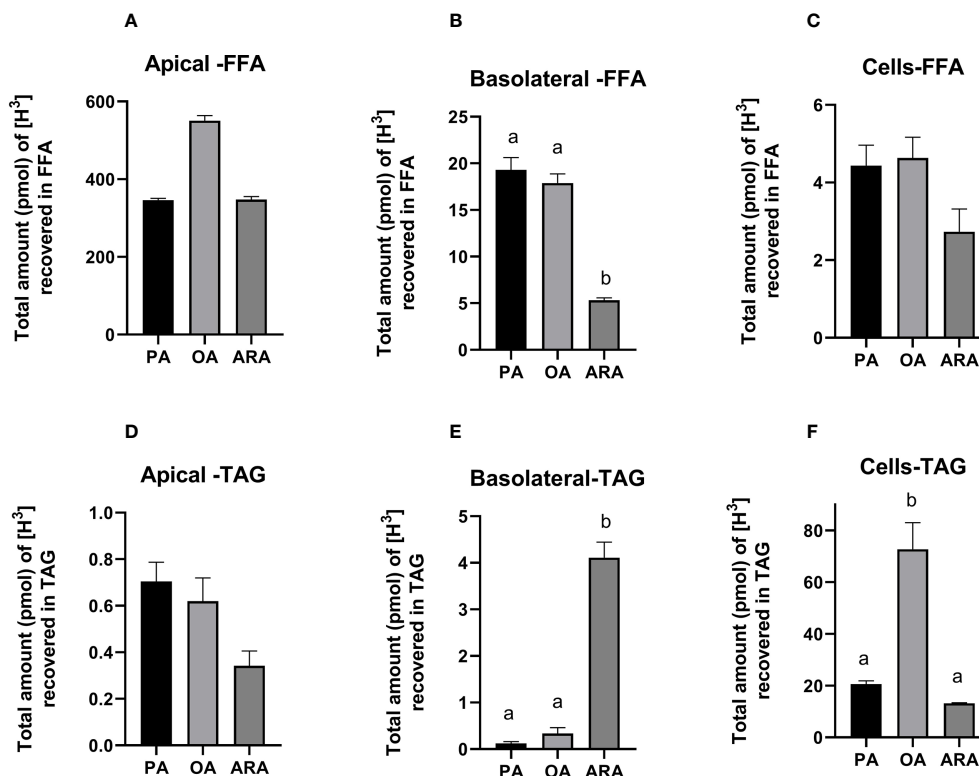


FIGURE 5

Lipid class analysis of RTgutGC cells grown on transwell membrane inserts for 18 days and then exposed to [³H] labelled FAs (PA, OA or ARA) for 16 h at 19°C. FFA from apical (A), basolateral (B) and the cells fractions (C); TAG from apical (D), basolateral (E) and the cell fractions (F) measured as the total amount (pmol) of [³H] recovered after scintillation counting. Different superscript (small letters) indicates statistical significance as obtained through one-way ANOVA followed by Tukey's multiple comparisons. Data from two independent experiments in triplicate (N=2; n=3) and are shown as mean ± SEM. PA, Palmitic acid; ARA, Arachidonic acid; OA, Oleic acid; TAG, Triacylglycerides.

Discussion

In the current study, we demonstrated how the absorption and intracellular trafficking of FAs vary according to their carbon chain length and saturation level in the RTgutGC cell line. To the best of our knowledge, the present study is the first of its kind using a fish enterocyte cell line as a model to investigate the intracellular fates of different FAs. However, a human intestinal Caco2 cell line, derived from colorectal adenocarcinoma, has been extensively used as an enterocyte cell model to study the mechanism of FAs absorption and intracellular transport (Ranheim et al., 1994; Van Greevenbroek et al., 1995; Trotter et al., 1996; Nauli and Whittimore, 2015). The majority of the studies in Caco2 cells have demonstrated that MUFA (OA) induced a higher rate of TAG synthesis and CLDs than SFA and PUFA (Field et al., 1988; Dashti et al., 1990; Levin et al., 1992; Bateman et al., 2007), thus explaining that each FA has its own fate inside the enterocyte according to their chain length and degree of saturation (Yonezawa et al., 2004b; Vargas-Bello-Pérez et al., 2019). Similarly, OA-induced CLD accumulation has also been observed in other cell types such

as HepG2 hepatocytes (Eynaoui et al., 2021), pancreatic β-cells (Cnop et al., 2001), bovine mammary epithelial cells (Yonezawa et al., 2004a) and H9C2 cardiomyoblasts (Akoumi et al., 2017). *In vitro* studies in adipocytes isolated from Atlantic salmon have demonstrated the increased CLDs in response to OA treatment (Todorčević et al., 2008; Bou et al., 2020). In addition to *in vitro* studies, several *in vivo* studies in fish have shown similar mechanisms of excessive LD accumulation in intestinal tissue in response to diets containing vegetable oils high in MUFA (Fontagné et al., 1998; Olsen et al., 1999; Olsen et al., 2000; Caballero et al., 2002; Caballero et al., 2003; Olsen et al., 2003). In accordance with these reports, in the present study we also observed a higher rate of TAG synthesis and subsequent CLD accumulation in OA treated cells. Hence, the RTgutGC cells respond similarly as other well-tested cell lines and *in vivo* studies, and it is deemed to be a suitable enterocyte model to investigate the intracellular fate of individual FAs.

Long chain fatty acid (LCFA) transported into cells are acylated into long-chain acyl-CoA by the action of acyl-CoA synthetases and are then destined for either TAG synthesis or β-

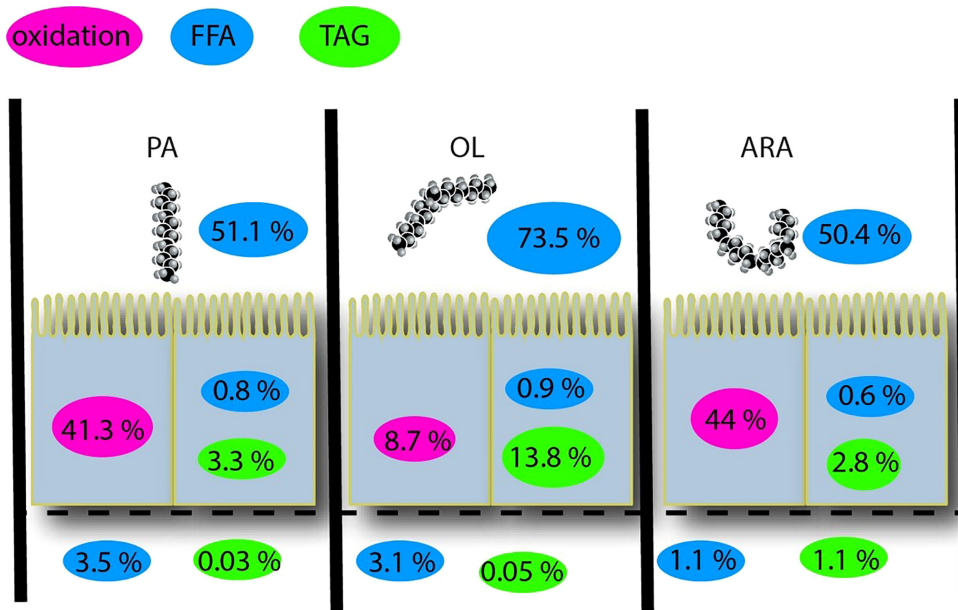


FIGURE 6
Summary of percentage of FFA and TAG in different compartment of RTgutGC cells grown on transwell membrane inserts for 18 days and then exposed to [³H] labelled FAs (PA, OA or ARA) for 16 h at 19°C. FA, Fatty acid; PA, Palmitic acid; OA, Oleic acid; ARA, Arachidonic acid; TAG, Triacylglycerides; CLDs, cytosolic lipid droplets. Ox, β-Oxidation.

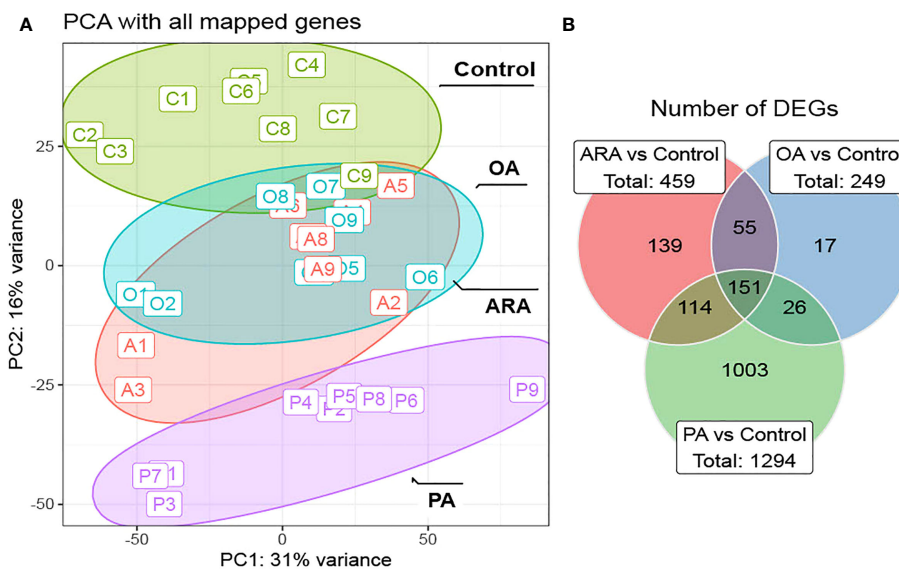
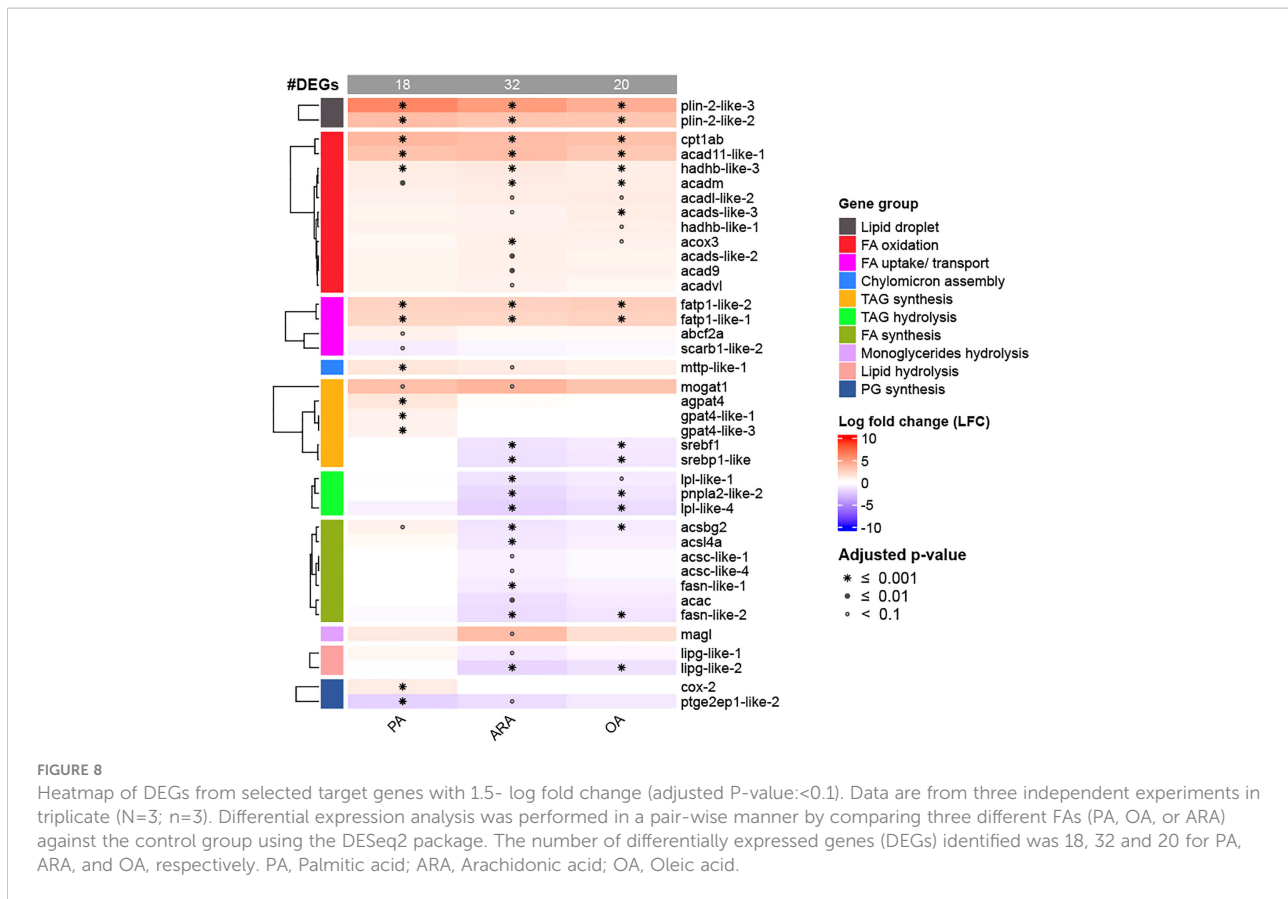


FIGURE 7
Transcriptomics analysis of RTgutGC cells treated with 200 μM of FAs (PA, OA or ARA) control for 16 h at 19°C. (A) PCA biplot of differentially expressed genes of RNAseq counts. (B) Venn diagram depicting the number of common and unique genes showing differential expression in PA, OA and ARA treatment groups. 1.5- log fold change (adjusted P-value of 0.01). Differential expression analysis was performed in a pair-wise manner by comparing three different FAs (PA, OA, or ARA) against the control group using the DESeq2 package. Data are from three independent experiments in triplicate (N=3; n=3). PA, Palmitic acid; ARA, Arachidonic acid; OA, Oleic acid.



oxidation (Listenberger et al., 2003). We hypothesized that the fish enterocyte metabolizes PA, OA and ARA differently and that they are stored temporarily as CLDs before being exported to circulation as chylomicrons/VLDL (very low-density lipoprotein). This appears to be true for OA, where we found increased CLD accumulation, although the possible underlying mechanisms remain unclear. Phospholipids and lipoproteins are important components of chylomicrons/VLDL, thus enabling the transport of lipids. Recently, an *in vivo* study in fish has demonstrated that diets deficient in phospholipids leads to accumulation of CLDs, hypothesized to be caused by insufficient lipoprotein synthesis (Gu et al., 2014; Sæle et al., 2018). Furthermore, an earlier study in gilthead seabream (*Sparus aurata*) fed a rapeseed diet containing high amount of OA (46% of total FAs) observed reduced lipoprotein synthesis rates compared to diets lower in OA. They also found lower re-cyclation of OA in the phospholipid fraction, suggested to be the reason behind reduced lipoprotein synthesis (Caballero et al., 2003). Hence, one could easily speculate that insufficient lipoprotein synthesis might be one possible reason for the increased CLD accumulation. However, these studies are conducted *in vivo*, where dietary lipid sources are complex mixtures of FAs and lipid classes. In contrast, in the current *in*

vitro study, cells were exposed to individual FAs (PA, OA, or ARA) complexed with BSA, meaning that phospholipid level must be the same for all groups. This leads us to question why OA would require more phospholipids than other FAs (PA and ARA) to form chylomicrons/VLDL. The mechanisms behind this remain unclear and need to be addressed in future studies.

Conversely, the lower accumulation of CLDs for PA and ARA might indicate that they are preferentially used for β -oxidation instead of TAG synthesis and LD storage or phospholipid synthesis. This is further supported by quantitative data, where 91% of FAs was recovered for OA, but only 58% of PA and 56% were recovered for PA and ARA, respectively. PA is an important component of phosphatidylcholine (PC) and is required for lipoprotein synthesis (Bell et al., 1985; Olsen et al., 2000). Similarly, PUFAs such as EPA, DHA and ARA are preferentially esterified into phospholipids than less unsaturated FA like OA. This is probably due to their essential function to maintain membrane integrity and functionality of the cells biomembrane (Bell et al., 1985). Therefore, some amount of PA and ARA might be acylated into the phospholipid fractions. Unfortunately, we did not measure the recovered radioactivity in β -oxidation products or the phospholipid fraction and hence

can only speculate that this was the fate of these FA. However, in support of our speculation, an *in vitro* study in the HepG2 cell line demonstrated that PA preferably stimulates mitochondrial oxidative metabolism, while OA results in abundant CLDs with a slower mitochondrial oxidation (Eynaudi et al., 2021). Similarly, a study on isolated hepatocytes from Atlantic salmon reported that ARA, followed by PA were the preferential substrates for β -oxidation compared to OA (Stubhaug et al., 2005). In the present study, significantly lower recovery of [3 H] FA for PA and ARA compared to OA, might indicate enhanced β -oxidation of these FA. However, the expression of genes related to β -oxidation does not show any significant difference between FA. Furthermore, the cells that are exposed to high FFA concentrations cause ER stress which may lead to cell dysfunction, and apoptosis (Cui et al., 2013). However, in the present study we did not observe upregulation of transcripts involved in ER stress (*edem*, *hsp70*).

Additionally, our study showed that OA not only increases the CLDs accumulation, but it also promotes CLDs with larger volume, surface and diameter. This is probably due to fusion of CLDs, assumed to be mediated through members of the SNARE protein family (Boström et al., 2007). Although it is generally accepted that formation of large CLDs protects the cell from lipotoxic effects from excess FFA (Bateman et al., 2007; Ricchi et al., 2009; Eynaudi et al., 2021). However, the formation of large CLDs along with excessive accumulation in intracellular space may also lead to cell dysfunction or cell death (Schaffer, 2003). Accordingly, several *in vivo* studies in fish have demonstrated extensive damage to enterocytes caused by high lipid accumulation (Deplano et al., 1989; Olsen et al., 1999; Olsen et al., 2000). Our study demonstrated that OA contributes to lipid accumulation in enterocytes through increased number and size of CLDs, suggesting that dietary inclusion of OA rich oils should be limited.

The perilipins, encoded by the *plin* genes, are the major proteins associated to CLD surface that regulate lipid droplet stability and turnover (Ko et al., 2020). Among reported *plin* (*plin1*, *plin2*, *plin3*, and *plin6*) in fish, including rainbow trout, *plin2* is ubiquitously expressed in all tissue and is associated with increased CLDs accumulations. In addition, the microsomal triglyceride transfer protein (*mtp*), primarily involved in lipoprotein assembly and also reported to be present in CLDs, has been found to increase as a response to excessive CLD accumulation (Love et al., 2015). In the current study, all three FA types triggered the overexpression of *plin2* and *mtp* transcripts compared to the control. However, the expression was significantly higher for PA followed by ARA and OA, which is not correlated with the CLDs observed from image analysis. Similar patterns were also observed for the transcripts involved in the TAG pathway (*mogat*, *agpat4*). A recent study by Etayo et al. (2021) in ballan wrasse (*Labrus bergylta*) fed lipid rich meal, reported the initial increase in gene expression involved in serotonin synthesis and then declined over time post-prandially.

Simultaneously, serotonin (5-HT) levels increased in the same tissues. A highly abundant protein will usually have a highly expressed mRNA. Nevertheless, there are factors involved in the process between gene transcription and translation into protein, which can result in a mismatch between gene expression and protein level. For example, the half-life of different proteins can vary from minutes to days, whereas mRNA degrades within hours (Hargrove and Schmidt, 1989). Other possible factors include the lower rate of mRNA transcription than protein translation and possible negative feedback mechanisms, which might also have contributed to the currently observed lack of correlation between mRNA transcripts and CLDs accumulation. A further study with time series samplings could provide additional information in regulations at transcriptional levels.

FA chain length and degree of saturation influence the uptake by intestinal cells (Wang et al., 2013). However, the way it is regulated also depends on several other factors including the number of monomers delivered, membrane solubility, permeability of monolayer, and membrane carrier protein activity (*fabp*, scavenger *cd36*, *fatp*). In the present study, the mean uptake of labelled OA from the apical compartment was significantly lower than the other FAs, which is concurrent with the increased number and size of CLDs observed. Thus, this result might indicate that excessive accumulation of CLDs in the cytosol may present a physical barrier and cause the lower cellular uptake for this OA (Morais et al., 2007). On the other hand, the uptake of PA and ARA from the apical compartment by cells was quite efficient. The greater uptake of PA may be due to lower water solubility and the greater membrane solubility of PA compared to OA or could also be caused by a greater efficiency of carrier protein (*fabp* and scavenger *cd36*, *fatp*) in transporting PA compared to OA, despite similar affinity for PA and OA (Trotter et al., 1996). Furthermore, the higher affinity of cytosolic FABP and higher esterification rate for PUFA (Sire et al., 1981; Pérez et al., 1999) could possibly explain the better uptake of complex FAs like ARA.

To transport re-esterified FA (TAG) from enterocytes to systemic circulation and to peripheral tissues, TAG must be incorporated into lipoproteins (*apob*, *apoa1*, *apoa4*, *apoc*, *apoe*, and *apod*). The *apob* is a major secretory lipoprotein, and its role in transporting TAG from enterocytes to circulation is well recognized. Previous studies in caco2 cells have clearly demonstrated the expression of *apob* both in the presence or absence of FAs supplements (Liao and Chan, 2000; Bateman et al., 2007). Similarly, the induction of *apob* expression in response to diets has also been demonstrated in the fish intestine, including rainbow trout (Kamalam et al., 2013a; Kamalam et al., 2013b). However, in the current study, we observed very low expression of *apob*, and although other apolipoproteins (*apoa1*, *apoa4*, *apoc*, *apoe*, and *apod*) were expressed, no DEGs for any of these apolipoproteins in all treatment groups, including control. This might be related to

the time points at which the cells were sampled after FAs exposure as described in [Etayo et al. \(2021\)](#).

While it has been widely accepted that LCFAs are transported mainly as esterified form (TAG), in the present study, we observed a significant amount of fatty acids as FFA in the basolateral region in the PA and OA treatments, but also some in the ARA group. A possible explanation for this could be that the high amount of FA load in the apical region might cause transport of a certain amount of these FFA directly into the basolateral chamber (and into circulation). Similar results have been observed *in vivo* in Atlantic salmon ([Denstadli et al., 2011](#)), where they reported the transport of OA both as esterified lipids (TAG) as well as FFA form in portal blood. Similarly, an earlier study by [Kayama and Iijima \(1976\)](#) in carp fed radiolabeled PA found significant amount of labelled FFA in the circulation and suggested that the FFA plays an important role in fish lipid transport system. Similarly, in the current study, for the more complex FA like ARA, the amount of recovered FFA in the basolateral fraction was quite low compared to PA and OA. On the other hand, the TAG amount in the basolateral fraction was significantly higher for ARA than others. These results might indicate a better regulated intracellular transport of complex FAs like ARA.

Conclusion

The present study demonstrated that RTgutGC cells have the characteristics of absorbing and transporting the FA, which is comparable to similar mammalian cell lines as well as *in vivo* studies in fish or mammals. Thus, RTgutGC could serve as a suitable *in vitro* model to study the intracellular trafficking of fatty acids and their metabolism. As hypothesized, carbon-chain length and saturation level of FA differently regulate the TAG synthesis and subsequent CLDs accumulation, where the accumulation of TAG in CLDs was higher for oleic acid (OA) compared to arachidonic acid (ARA) and palmitic acid (PA). Accumulation of CLDs negatively affected the absorption of FA into the cells, such that PA and ARA are better absorbed by the cells than OA. The relatively higher amount of FFA being transported to the serosal basolateral side for PA and OA is backed up by findings *in vivo* in fish. The lower recovery of radiolabeled FA for PA might suggest that PA and ARA are preferred substrates for β -oxidation over OA, warranting further understanding of intestinal lipid transport in teleost.

Data availability statement

The datasets presented in this study can be found in online repositories. The names of the repository/repositories and accession number(s) can be found in the article/[Supplementary Material](#).

Author contributions

CS- the main author of the manuscript, conducted the experiments, data analysis, and wrote the manuscript. TS- carried out Transcriptomics analysis. NS- conceived and planned the experiments AP- conceived and planned the experiments. OS - conceived, designed, and coordinated the study. All authors contributed to the article and approved the submitted version.

Funding

This study was funded by The Ministry of Industry, Trade and Fisheries, Norway through IMR (the Institute of Marine Research) under the project *NuFiMo* (15473, Nutrition in fish models).

Acknowledgments

Joar Breivik and Andrey Volynkin at the Institute of Marine Research are acknowledged for technical assistance in radioisotopes lab. The first author acknowledges the Indian Council of Agricultural Research, New Delhi, India, for providing PhD scholarship under Netaji Subhas-ICAR International Fellowship program and study leave by the Director, ICAR-Central Marine Fisheries Research Institute, India for the doctoral study.

Conflict of interest

The authors declare that the research was conducted in the absence of any commercial or financial relationships that could be construed as a potential conflict of interest.

Publisher's note

All claims expressed in this article are solely those of the authors and do not necessarily represent those of their affiliated organizations, or those of the publisher, the editors and the reviewers. Any product that may be evaluated in this article, or claim that may be made by its manufacturer, is not guaranteed or endorsed by the publisher.

Supplementary material

The Supplementary Material for this article can be found online at: <https://www.frontiersin.org/articles/10.3389/fmars.2022.954773/full#supplementary-material>

References

- Akoumi, A., Haffar, T., Moustherji, M., Kiss, R. S., and Bousette, N. (2017). Palmitate mediated diacylglycerol accumulation causes endoplasmic reticulum stress, Plin2 degradation, and cell death in H9C2 cardiomyoblasts. *Exp. Cell Res.* 354, 85–94. doi: 10.1016/j.yexcr.2017.03.032
- Antony Jesu Prabhu, P., Stewart, T., Silva, M., Amlund, H., Ornsrud, R., Lock, E. J., et al. (2018). Zinc uptake in fish intestinal epithelial model RTgutGC: Impact of media ion composition and methionine chelation. *J. Trace Elem. Med. Biol.* 50, 377–383. doi: 10.1016/j.jtemb.2018.07.025
- Bateman, P. A., Jackson, K. G., Maitin, V., Yaqoob, P., and Williams, C. M. (2007). Differences in cell morphology, lipid and apo b secretory capacity in caco-2 cells following long term treatment with saturated and monounsaturated fatty acids. *Biochim. Biophys. Acta (BBA) - Mol. Cell Biol. Lipids* 1771, 475–485. doi: 10.1016/j.bbailip.2007.02.001
- Bell, M. V., Henderson, R. J., and Sargent, J. R. (1985). Changes in the fatty acid composition of phospholipids from turbot (*Scophthalmus maximus*) in relation to dietary polyunsaturated fatty acid deficiencies. *Comp. Biochem. Physiol. Part B: Comp. Biochem.* 81, 193–198. doi: 10.1016/0305-0491(85)90182-8
- Berger, E., Nassra, M., Atgić, C., Plaisancié, P., and Géloën, A. (2017). Oleic acid uptake reveals the rescued enterocyte phenotype of colon cancer caco-2 by HT29-MTX cells in Co-culture mode. *Int. J. Mol. Sci.* 18, 1573. doi: 10.3390/ijms18071573
- Bogevik, A. S., Oxley, A., and Olsen, R. E. (2008). Hydrolysis of acyl-homogeneous and fish oil triacylglycerols using desalted midgut extract from Atlantic salmon, *Salmo salar*. *Lipids* 43, 655–662. doi: 10.1007/s11745-008-3185-2
- Boström, P., Andersson, L., Rutberg, M., Perman, J., Lidberg, U., Johansson, B. R., et al. (2007). SNARE proteins mediate fusion between cytosolic lipid droplets and are implicated in insulin sensitivity. *Nat. Cell Biol.* 9, 1286–1293. doi: 10.1038/ncb1648
- Bou, M., Wang, X., Todorčević, M., Østbye, T.-K. K., Torgersen, J., and Ruyter, B. (2020). Lipid deposition and mobilisation in Atlantic salmon adipocytes. *Int. J. Mol. Sci.* 21, 2332. doi: 10.3390/ijms21072332
- Caballero, M. J., Izquierdo, M. S., Kjorsvik, E., Montero, D., Socorro, J., Fernández, A. J., et al. (2003). Morphological aspects of intestinal cells from gilthead seabream (*Sparus aurata*) fed diets containing different lipid sources. *Aquaculture* 225, 325–340. doi: 10.1016/S0044-8486(03)00299-0
- Caballero, M. J., Obach, A., Rosenlund, G., Montero, D., Gisvold, M., and Izquierdo, M. S. (2002). Impact of different dietary lipid sources on growth, lipid digestibility, tissue fatty acid composition and histology of rainbow trout, *Oncorhynchus mykiss*. *Aquaculture* 214, 253–271. doi: 10.1016/S0044-8486(01)00852-3
- Cnop, M., Hannaert, J. C., Hoorens, A., Eizirik, D. L., and Pipeleers, D. G. (2001). Inverse relationship between cytotoxicity of free fatty acids in pancreatic islet cells and cellular triglyceride accumulation. *Diabetes* 50, 1771–1777. doi: 10.2337/diabetes.50.8.1771
- Cui, W., Ma, J., Wang, X., Yang, W., Zhang, J., and Ji, Q. (2013). Free fatty acid induces endoplasmic reticulum stress and apoptosis of β -cells by Ca²⁺/Calpain-2 pathways. *PLoS One* 8, e59921. doi: 10.1371/journal.pone.0059921
- Dashti, N., Smith, E. A., and Alaouie, P. (1990). Increased production of apolipoprotein b and its lipoproteins by oleic acid in caco-2 cells. *J. Lipid Res.* 31, 113–123. doi: 10.1016/S0022-2275(20)42765-8
- Denstadli, V., Bakke, A. M., Berge, G. M., Krogdahl, Å., Hillestad, M., Holm, H., et al. (2011). Medium-chain and long-chain fatty acids have different postabsorptive fates in Atlantic salmon. *J. Nutr.* 141, 1618–1628. doi: 10.3945/jn.111.141820
- Deplano, M., Connes, R., Diaz, J. P., and Paris, J. (1989). Intestinal steatosis in the farm-reared sea bass *dicentrarchus labrax*. *Dis. Aquat. Organism* 6, 121–130. doi: 10.3354/dao006121
- Dobin, A., Davis, C. A., Schlesinger, F., Drenkow, J., Zaleski, C., Jha, S., et al. (2013). STAR: Ultrafast universal RNA-seq aligner. *Bioinformatics* 29, 15–21. doi: 10.1093/bioinformatics/bts635
- Etayo, A., Le, H. T. M. D., Araujo, P., Lie, K. K., and Sæle, Ø. (2021). Dietary lipid modulation of intestinal serotonin in ballan wrasse (*Labrus bergyllta*)—*In vitro*. *Analyses. Front. Endocrinol.* 12, 560055. doi: 10.3389/fendo.2021.560055
- Eynaudi, A., Diaz-Castro, F., Bórquez, J. C., Bravo-Sagua, R., Parra, V., and Troncoso, R. (2021). Differential effects of oleic and palmitic acids on lipid droplet-mitochondria interaction in the hepatic cell line HepG2. *Front. Nutr.* 8, 775382. doi: 10.3389/fnut.2021.775382
- Field, F. J., Albright, E., and Mathur, S. N. (1988). Regulation of triglyceride-rich lipoprotein secretion by fatty acids in CaCo-2 cells. *J. Lipid Res.* 29, 1427–1437. doi: 10.1016/S0022-2275(20)38423-6
- Fontagné, S., Geurden, I., Escaffre, A.-M., and Bergot, P. (1998). Histological changes induced by dietary phospholipids in intestine and liver of common carp (*Cyprinus carpio* L.) larvae. *Aquaculture* 161, 213–223. doi: 10.1016/S0044-8486(97)00271-8
- Geppert, M., Sigg, L., and Schirmer, K. (2016). A novel two-compartment barrier model for investigating nanoparticle transport in fish intestinal epithelial cells. *Environ. Sci. Nano* 3, 388–395. doi: 10.1039/C5EN00226E
- Gu, Z., Eils, R., and Schlesner, M. (2016). Complex heatmaps reveal patterns and correlations in multidimensional genomic data. *Bioinformatics* 32, 2847–2849. doi: 10.1093/bioinformatics/btw313
- Gu, M., Kortner, T. M., Penn, M., Hansen, A. K., and Krogdahl, Å. (2014). Effects of dietary plant meal and soya-saponin supplementation on intestinal and hepatic lipid droplet accumulation and lipoprotein and sterol metabolism in Atlantic salmon (*Salmo salar* L.). *Br. J. Nutr.* 111, 432–444. doi: 10.1017/S0007114513002717
- Hargrove, J. L., and Schmidt, F. H. (1989). The role of mRNA and protein stability in gene expression. *FASEB J.* 3, 2360–2370. doi: 10.1096/fasebj.3.12.2676679
- Holen, E., Austgulen, M. H., and Espe, M. (2021). RNA Form baker's yeast cultured with and without lipopolysaccharide (LPS) modulates gene transcription in an intestinal epithelial cell model, RTgutGC from rainbow trout (*Oncorhynchus mykiss*). *Fish Shellfish Immunol.* 119, 397–408. doi: 10.1016/j.fsi.2021.10.018
- Kamalam, B. S., Médale, F., Larroquet, L., Corraze, G., and Panserat, S. (2013a). Metabolism and fatty acid profile in fat and lean rainbow trout lines fed with vegetable oil: effect of carbohydrates. *PLoS One* 8, e76570–e76570. doi: 10.1371/journal.pone.0076570
- Kamalam, B. S., Panserat, S., Aguirre, P., Geurden, I., Fontagné-Dicharry, S., and Médale, F. (2013b). Selection for high muscle fat in rainbow trout induces potentially higher chylomicron synthesis and PUFA biosynthesis in the intestine. *Comp. Biochem. Physiol. Part A: Mol. Integr. Physiol.* 164, 417–427. doi: 10.1016/j.cbpa.2012.11.020
- Kawano, A., Haiduk, C., Schirmer, K., Hanner, R., Lee, L. E. J., Dixon, B., et al. (2011). Development of a rainbow trout intestinal epithelial cell line and its response to lipopolysaccharide. *Aquacult. Nutr.* 17, e241–e252. doi: 10.1111/j.1365-2095.2010.00757.x
- Kayama, M., and Iijima, N. (1976). Studies on lipid transport mechanism in the fish. *Bull. Japanese Soc. Sci. Fish* 42, 987–996. doi: 10.2331/suisan.42.987
- Kim, J. J., Pham, P. H., Hamilton, M. E., Lee, L. E. J., and Bols, N. C. (2018). Effect of selenomethionine on cell viability and heat shock protein 70 levels in rainbow trout intestinal epithelial cells at hypo-, normo-, and hyper-thermic temperatures. *J. Thermal Biol.* 76, 107–114. doi: 10.1016/j.jtherbio.2018.07.011
- Ko, C. W., Qu, J., Black, D. D., and Tso, P. (2020). Regulation of intestinal lipid metabolism: current concepts and relevance to disease. *Nat. Rev. Gastroenterol. Hepatol.* 17, 169–183. doi: 10.1038/s41575-019-0250-7
- Koster, J., and Rahmann, S. (2012). Snakemake—a scalable bioinformatics workflow engine. *Bioinformatics* 28, 2520–2522. doi: 10.1093/bioinformatics/bts480
- Langan, L. M., Harper, G. M., Owen, S. F., Purcell, W. M., Jackson, S. K., and Jha, A. N. (2017). Application of the rainbow trout derived intestinal cell line (RTgutGC) for ecotoxicological studies: Molecular and cellular responses following exposure to copper. *Ecotoxicology* 26, 1117–1133. doi: 10.1007/s10646-017-1838-8
- Levin, M. S., Talkad, V. D., Gordon, J. I., and Stenson, W. F. (1992). Trafficking of exogenous fatty acids within caco-2 cells. *J. Lipid Res.* 33, 9–19. doi: 10.1016/S0022-2275(20)41878-4
- Liao, W., and Chan, L. (2000). Apolipoprotein b, a paradigm for proteins regulated by intracellular degradation, does not undergo intracellular degradation in CaCo2 cells. *J. Biol. Chem.* 275, 3950–3956. doi: 10.1074/jbc.275.6.3950
- Liao, Y., Smyth, G. K., and Shi, W. (2014). featureCounts: An efficient general purpose program for assigning sequence reads to genomic features. *Bioinformatics* 30, 923–930. doi: 10.1093/bioinformatics/btt656
- Listenberger, L. L., Han, X., Lewis, S. E., Cases, S., Farese, R. V., Ory, D. S., et al. (2003). Triglyceride accumulation protects against fatty acid-induced lipotoxicity. *Proc. Natl. Acad. Sci. U.S.A.* 100, 3077–3082. doi: 10.1073/pnas.0630588100
- Love, M. I., Huber, W., and Anders, S. (2014). Moderated estimation of fold change and dispersion for RNA-seq data with DESeq2. *Genome Biol.* 15, 550. doi: 10.1186/s13059-014-0550-8
- Love, J. D., Suzuki, T., Robinson, D. B., Harris, C. M., Johnson, J. E., Mohler, P. J., et al. (2015). Microsomal triglyceride transfer protein (MTP) associates with cytosolic lipid droplets in 3T3-L1 adipocytes. *PLoS One* 10, e0135598–e0135598. doi: 10.1371/journal.pone.0135598

- Martin, M. (2011). Cutadapt removes adapter sequences from high-throughput sequencing reads. *EMBnetjournal* 17, 10–12. doi: 10.14806/ej.17.1.200
- Minghetti, M., Drieschner, C., Bramaz, N., Schug, H., and Schirmer, K. (2017). A fish intestinal epithelial barrier model established from the rainbow trout (*Oncorhynchus mykiss*) cell line, RTgutGC. *Cell Biol. Toxicol.* 33, 539–555. doi: 10.1007/s10565-017-9385-x
- Morais, S., Conceição, L. E. C., Rønnestad, I., Koven, W., Cahu, C., Zambonino Infante, J. L., et al. (2007). Dietary neutral lipid level and source in marine fish larvae: Effects on digestive physiology and food intake. *Aquaculture* 268, 106–122. doi: 10.1016/j.aquaculture.2007.04.033
- Nøstbakken, O. J., Goksoyr, A., Martin, S., Cash, P., and Torstensen, B. E. (2012). Marine n-3 fatty acids alter the proteomic response to methylmercury in Atlantic salmon kidney (ASK) cells. *Aquat. Toxicol.* 106–107, 65–75. doi: 10.1016/j.aquatox.2011.10.008
- Nauli, A. M., and Whittimore, J. D. (2015). Using caco-2 cells to study lipid transport by the intestine. *J. visualized experiments JoVE*. 102, e53086. doi: 10.3791/53086
- Olsen, R. E., Myklebust, R., Kaino, T., and Ringø, E. (1999). Lipid digestibility and ultrastructural changes in the enterocytes of Arctic char (*Salvelinus alpinus* L.) fed linseed oil and soybean lecithin. *Fish Physiol. Biochem.* 21, 35–44. doi: 10.1023/A:1007726615889
- Olsen, R. E., Myklebust, R., Ringø, E., and Mayhew, T. M. (2000). The influences of dietary linseed oil and saturated fatty acids on caecal enterocytes in Arctic char (*Salvelinus alpinus* L.): A quantitative ultrastructural study. *Fish Physiol. Biochem.* 22, 207–216. doi: 10.1023/A:1007879127182
- Olsen, R. E., Tore Dragnes, B., Myklebust, R., and Ringø, E. (2003). Effect of soybean oil and soybean lecithin on intestinal lipid composition and lipid droplet accumulation of rainbow trout, *oncorhynchus mykiss* Walbaum. *Fish Physiol. Biochem.* 29, 181–192. doi: 10.1023/B:FISH.0000045708.67760.43
- Olzmann, J. A., and Carvalho, P. (2019). Dynamics and functions of lipid droplets. *Nat. Rev. Mol. Cell Biol.* 20, 137–155. doi: 10.1038/s41580-018-0085-z
- Pérez, J. A., Rodríguez, C., and Henderson, R. J. (1999). The uptake and esterification of radiolabelled fatty acids by enterocytes isolated from rainbow trout (*Oncorhynchus mykiss*). *Fish Physiol. Biochem.* 20, 125–134. doi: 10.1023/A:1007795516689
- Pumputis, P. G., Dayeh, V. R., Lee, L. E. J., Pham, P. H., Liu, Z., Vithiyapaskaran, S., et al. (2018). Responses of rainbow trout intestinal epithelial cells to different kinds of nutritional deprivation. *Fish Physiol. Biochem.* 44, 1197–1214. doi: 10.1007/s10695-018-0511-3
- Ranheim, T., Gedde-Dahl, A., Rustan, A. C., and Drevon, C. A. (1994). Fatty acid uptake and metabolism in CaCo-2 cells: Eicosapentaenoic acid (20:5(n-3)) and oleic acid (18:1(n-9)) presented in association with micelles or albumin. *Biochim. Biophys. Acta* 1212, 295–304. doi: 10.1016/0005-2760(94)90203-8
- Ricchi, M., Odoardi, M. R., Carulli, L., Anzivino, C., Ballestri, S., Pinetti, A., et al. (2009). Differential effect of oleic and palmitic acid on lipid accumulation and apoptosis in cultured hepatocytes. *J. Gastroenterol. Hepatol.* 24, 830–840. doi: 10.1111/j.1440-1746.2008.05733.x
- Sæle, Ø., Rød, K. E. L., Quinlivan, V. H., Li, S., and Farber, S. A. (2018). A novel system to quantify intestinal lipid digestion and transport. *Biochim. Biophys. Acta (BBA) - Mol. Cell Biol. Lipids* 1863, 948–957. doi: 10.1016/j.bbalip.2018.05.006
- Schaffer, J. E. (2003). Lipotoxicity: when tissues overeat. *Curr. Opin. Lipidol.* 14 (3), 281–287. doi: 10.1097/00041433-200306000-00008
- Schug, H., Maner, J., Hulskamp, M., Begnaud, F., Debonneville, C., Berthaud, F., et al. (2020). Extending the concept of predicting fish acute toxicity *in vitro* to the intestinal cell line RTgutGC. *ALTEX* 37, 37–46. doi: 10.14573/altex.1905032
- Sheridan, M. A. (1988). Lipid dynamics in fish: Aspects of absorption, transportation, deposition and mobilization. *Comp. Biochem. Physiol. Part B: Comp. Biochem.* 90, 679–690. doi: 10.1016/0305-0491(88)90322-7
- Sigurisdottir, S., Lall, S. P., Parrish, C. C., and Ackman, R. G. (1992). Cholestane as a digestibility marker in the absorption of polyunsaturated fatty acid ethyl esters in Atlantic salmon. *Lipids* 27, 418. doi: 10.1007/BF02536382
- Sire, M. F., Lutton, C., and Vernier, J. M. (1981). New views on intestinal absorption of lipids in teleostean fishes: An ultrastructural and biochemical study in the rainbow trout. *J. Lipid Res.* 22, 81–94. doi: 10.1016/S0022-2275(20)34743-X
- Stubhaug, I., Tocher, D. R., Bell, J. G., Dick, J. R., and Torstensen, B. E. (2005). Fatty acid metabolism in Atlantic salmon (*Salmo salar* L.) hepatocytes and influence of dietary vegetable oil. *Biochim. Biophys. Acta (BBA) - Mol. Cell Biol. Lipids* 1734, 277–288. doi: 10.1016/j.bbalip.2005.04.003
- Todorčević, M., Vegusdal, A., Gjøen, T., Sundvold, H., Torstensen, B. E., Kjaer, M. A., et al. (2008). Changes in fatty acids metabolism during differentiation of Atlantic salmon preadipocytes; effects of n-3 and n-9 fatty acids. *Biochim. Biophys. Acta* 1781, 326–335. doi: 10.1016/j.bbalip.2008.04.014
- Trotter, P. J., Ho, S. Y., and Storch, J. (1996). Fatty acid uptake by caco-2 human intestinal cells. *J. Lipid Res.* 37, 336–346. doi: 10.1016/S0022-2275(20)37620-3
- Van Greevenbroek, M. M., Voorhout, W. F., Erkelens, D. W., Van Meer, G., and De Bruin, T. W. (1995). Palmitic acid and linoleic acid metabolism in caco-2 cells: different triglyceride synthesis and lipoprotein secretion. *J. Lipid Res.* 36, 13–24. doi: 10.1016/S0022-2275(20)39750-9
- Vargas-Bello-Pérez, E., Loor, J. J., and Garnsworthy, P. C. (2019). Effect of different exogenous fatty acids on the cytosolic triacylglycerol content in bovine mammary cells. *Anim. Nutr.* 5, 202–208. doi: 10.1016/j.aninu.2018.09.002
- Walther, T. C., and Farese, R. V. Jr. (2012). Lipid droplets and cellular lipid metabolism. *Annu. Rev. Biochem.* 81, 687–714. doi: 10.1146/annurev-biochem-061009-102430
- Wang, J., Lei, P., Gamil, A., Lagos, L., Yue, Y., Schirmer, K., et al. (2019). Rainbow trout (*Oncorhynchus mykiss*) intestinal epithelial cells as a model for studying gut immune function and effects of functional feed ingredients. *Front. Immunol.* 10, 152. doi: 10.3389/fimmu.2019.00152
- Wang, T. Y., Liu, M., Portincasa, P., and Wang, D. Q. H. (2013). New insights into the molecular mechanism of intestinal fatty acid absorption. *Eur. J. Clin. Invest.* 43, 1203–1223. doi: 10.1111/eci.12161
- Yonezawa, T., Yonekura, S., Kobayashi, Y., Hagino, A., Katoh, K., and Obara, Y. (2004a). Effects of long-chain fatty acids on cytosolic triacylglycerol accumulation and lipid droplet formation in primary cultured bovine mammary epithelial cells. *J. Dairy Sci.* 87, 2527–2534. doi: 10.3168/jds.S0022-0302(04)73377-9
- Yonezawa, T., Yonekura, S., Sanosaka, M., Hagino, A., Katoh, K., and Obara, Y. (2004b). Octanoate stimulates cytosolic triacylglycerol accumulation and CD36 mRNA expression but inhibits acetyl coenzyme a carboxylase activity in primary cultured bovine mammary epithelial cells. *J. Dairy Res.* 71 398 – 404. doi: 10.1017/S0022029904000408